RDM1, a Novel RNA Recognition Motif (RRM)-containing Protein Involved in the Cell Response to Cisplatin in Vertebrates*

Received for publication, November 15, 2004, and in revised form, December 10, 2004 Published, JBC Papers in Press, December 14, 2004, DOI 10.1074/jbc.M412874200

Samia Hamimes‡§, Hiroshi Arakawa§¶, Alicja Z. Stasiak∥, Andrzej M. Kierzek**‡‡, Seiki Hirano§§, Yun-Gui Yang‡, Minoru Takata§§, Andrzej Stasiak∥, Jean-Marie Buerstedde¶, and Eric Van Dyck‡¶¶

From the ‡International Agency for Research on Cancer, 150 Cours Albert Thomas, 69372 Lyon, France, ¶Institute for Molecular Radiobiology, GSF, Ingolstaedter Landstrasse 1, D-85764 Neuherberg-Munich, Germany, ||Laboratoire d'Analyse Ultrastructurale, Université de Lausanne, 1015 Lausanne, Switzerland, **SBMS, University of Surrey, Guildford GU2 7XH, United Kingdom, §§Immunology and Molecular Genetics, Kawasaki Medical School, 577 Matsushima, Kurashiki, Okayama 701-0192, Japan, and ‡‡Institute of Biochemistry and Biophysics, Polish Academy of Sciences, Pawinskiego 5A, 02-106 Warsaw, Poland

A variety of cellular proteins has the ability to recognize DNA lesions induced by the anti-cancer drug cisplatin, with diverse consequences on their repair and on the therapeutic effectiveness of this drug. We report a novel gene involved in the cell response to cisplatin in vertebrates. The RDM1 gene (for RAD52 Motif 1) was identified while searching databases for sequences showing similarities to RAD52, a protein involved in homologous recombination and DNA double-strand break repair. Ablation of RDM1 in the chicken B cell line DT40 led to a more than 3-fold increase in sensitivity to cisplatin. However, RDM1^{-/-} cells were not hypersensitive to DNA damages caused by ionizing radiation, UV irradiation, or the alkylating agent methylmethane sulfonate. The RDM1 protein displays a nucleic acid binding domain of the RNA recognition motif (RRM) type. By using gel-shift assays and electron microscopy, we show that purified, recombinant chicken RDM1 protein interacts with single-stranded DNA as well as doublestranded DNA, on which it assembles filament-like structures. Notably, RDM1 recognizes DNA distortions induced by cisplatin-DNA adducts in vitro. Finally, human RDM1 transcripts are abundant in the testis, suggesting a possible role during spermatogenesis.

The cytotoxic activity of cisplatin (*cis*-diamminedichloroplatinum (II)) is thought to be due to its interaction with purine bases of our chromosomes and the various DNA adducts that ensue, including monoadducts and interstrand cross-links (ICLs), ¹ as well as the predominant (1,3- and 1,2-) intrastrand cross-links (1, 2). Cisplatin-DNA adducts perturb replication and transcription and trigger sophisticated repair machineries.

Cisplatin-DNA adducts are removed primarily by nucleotide excision repair (NER), which also operates in the repair of UV-induced lesions, DNA cross-links of various origins, and bulky DNA adducts (3, 4). NER has been elucidated thanks in part to the use of cell lines derived from patients with xeroderma pigmentosum (XP) and Cockayne syndrome (CS), in which NER was found to be deficient (5). NER has been subdivided in two subpathways that operate either on the transcribed strand of transcriptionally active genes (transcriptioncoupled repair (TCR)) or on the nontranscribed strand of active genes and in transcriptionally silent regions of the genome (global genome repair (GGR)) (6). The main difference between these pathways resides in the mechanisms by which they achieve specific recognition of a DNA lesion. In GGR, damage recognition involves the XPC-hHR23B complex, XPA, and RPA (7, 8), as well as the UV-damaged DNA binding complex (DDB) (9). In TCR, DNA damage is sensed by the RNA polymerase II, and repair is engaged by the transcription-coupled repair-specific factors CSA and CSB. Recognition of the lesion is followed by the sequential recruitment of proteins that mediate stages of repair common to GGR and TCR as follows: formation of an open, "pre-incision" complex, excision of a DNA fragment containing the lesion, and repair DNA synthesis (10). Although NER is the main pathway for the removal of intrastrand DNA cross-links, the molecular mechanisms that ensure repair of ICLs are still unclear. Current models suggest that such repair is initiated by DNA double-stranded breaks (DSBs) that are generated by the collapse of replication forks at the sites of lesion. These breaks are then acted upon by components of the NER and homologous recombination (HR) pathways, leading to the removal of the lesion (11). Biochemical evidence of DNA replication-mediated DSBs at sites of cross-links has been reported recently (12).

Removal of cisplatin-DNA cross-links contributes to resistance of tumors to the drug, a phenomenon frequently manifested during chemotherapy (2). Thus, increased expression of

cleotide excision repair; CS, Cockayne syndrome; dsDNA, double-stranded DNA; DSB, double-stranded break; GGR, global genome repair; HMG, high mobility group; HR, homologous recombination; MMR, mismatch repair; MMS, methylmethane sulfonate; ORF, open reading frame; RRM, RNA recognition motif; SSA, single-strand annealing; ssDNA, single-stranded DNA; TCR, transcription-coupled repair; XP, xeroderma pigmentosum; IPTG, isopropyl 1-thio-β-D-galactopyranoside; MES, 4-morpholineethanesulfonic acid; aa, amino acid.

^{*} This work was supported in part by grants from La Ligue Contre le Cancer, Comité du Rhône, l'Association pour la Recherche sur le Cancer, Grant BU 631/2–1 from the Deutsche Forschungsgemeinshaft, by the European Union Framework V Programs "Chicken Image" and "Genetics in a Cell Line," and by Grant 3100-058841 from the Swiss National Science Foundation. The costs of publication of this article were defrayed in part by the payment of page charges. This article must therefore be hereby marked "advertisement" in accordance with 18 U.S.C. Section 1734 solely to indicate this fact.

The nucleotide sequence(s) reported in this paper has been submitted to the DDBJ/GenBank $^{\rm TM}$ /EBI Data Bank with accession number(s) AB080727 and AB080728.

[§] Both authors contributed equally to this work.

^{¶¶} To whom correspondence should be addressed: Molecular Carcinogenesis, International Agency for Research on Cancer (IARC) 150 Cours Albert Thomas, 69732 Lyon, France. Tel.: 33-4-72-73-83-93; Fax: 33-4-72-73-83-23; E-mail: Vandyck@iarc.fr.

¹ The abbreviations used are: ICL, interstrand cross-links; NER, nu-

NER components and/or higher levels of cross-link excision activities have been detected in cancers that fail to respond to the drug (Ref. 13 and references therein). The efficiency of cisplatin-DNA lesion removal by NER has been shown to vary among different intrastrand cross-links, and biochemical studies have demonstrated that the major determinant in the efficiency of recognition and repair was the extent of structural distortion of the DNA caused by a given cross-link (14). It has been suggested that poor substrates for removal by NER, such as 1,2-intrastrand cross-links, tend to undergo replicative bypass, leading to the possible insertion of mispaired bases opposite the cross-links and the intervention of the mismatch repair (MMR) pathway. Consistent with this view, in vitro studies have shown that certain types of mismatched cisplatin-DNA adducts can be specifically recognized by the mismatch recognition complex hMutS α (15, 16). These observations may provide an explanation why MMR activity is compromised in certain cell lines selected for their resistance to cisplatin. It should be noted, however, that abrogation of MMR does not seem to occur frequently as a mechanism by which human cells acquire resistance to cisplatin (17).

In addition to the specific factors mentioned above, several other proteins, such as members of the high mobility group of proteins involved in chromatin compaction and gene expression, are capable of recognizing distortions of the double helix caused by cisplatin-DNA adducts (1, 2). In binding to such lesions, these proteins have the potential to mask the damaged DNA and prevent its repair or to recruit repair machineries, thereby facilitating the removal of the lesions. Hijacking effects, whereby binding of a factor to a cisplatin-DNA lesion is detrimental to other processes normally mediated by this factor, have also been suggested to concur to the cytotoxicity of cisplatin (18). The recognition of cisplatin-DNA lesions therefore appears to contribute greatly to the mechanisms by which cells express resistance to this drug.

Here we report a novel gene involved in the cell response to cisplatin in vertebrates. The RDM1 gene (for RAD52 Motif 1) was identified while searching databases for sequences showing similarities to the DNA recombination and repair gene RAD52 (Ref. 19 and Ref. 20 and references therein), by virtue of a small region of aa similarity, hereafter called the RD motif, that the RDM1 protein shares with a functionally important N-terminal region of RAD52. RDM1^{-/-} cells, generated by ablation of RDM1 in the chicken B cell line DT40, exhibited increased sensitivity to cisplatin. However, these cells were not hypersensitive to DNA damages caused by ionizing radiation, UV irradiation, or the alkylating agent methylmethane sulfonate (MMS). The RDM1 protein displays a nucleic-acid binding domain of the RNA recognition motif (RRM) type. By using gel-shift assays and electron microscopy, we show that purified, recombinant chicken RDM1 protein interacts with single-stranded DNA (ssDNA) as well as double-stranded DNA (dsDNA), on which it assembles filament-like structures. Most importantly, RDM1 was found to recognize distortions of the double helix induced by cisplatin-DNA adducts. Finally, high expression of human RDM1 transcripts was detected in the testis, suggesting that RDM1 might play a role during spermatogenesis.

EXPERIMENTAL PROCEDURES

DNA and Protein Sequence Analyses—Sequence similarity searches were carried out using the BLAST family of programs (21). The RRM motif of RDM1 was identified by using HHMER (22) to query the PFAM library of Hidden Markov models of protein families (23). The crystal structure of human RAD52 was examined using Swiss PDB Viewer (24). All programs were used with default parameters. Sequence data have been submitted to the DDBJ/GenBankTM/EBI Data Bank under accession numbers AB080727 (chicken RDM1) and AB080728 (human RDM1).

Cloning of the Chicken RDM1 Gene and Its Targeted Disruption in the Chicken B Cell Line DT40—The chicken RDM1 cDNA as well as its 5′ and 3′ regions were cloned using the SMART RACE cDNA amplification kit (Clontech). The genomic DNA fragments used to construct the RDM1 knock-out vectors were amplified using long range PCR, from DNA extracted from chicken DT40 cells. Gene disruption vectors (pRdm1Puro and pRdm1Bsr) were constructed as described previously (25). Recycling of the drug resistance markers was achieved using pLox vectors as described (26). DT40 cell culture, transfection, and genomic Southern blots were done as described previously (25).

DT40 Colony Survival Assay—The survival of DT40 cells in cisplatin- and MMS-containing medium was measured by plating serially diluted cells in chicken medium (25) containing 1% methylcellulose. Sensitivity to γ -radiation was measured by exposing plated cells to a $^{137}\mathrm{Cs}$ γ -ray source. UV irradiation (254 nm) was performed on cells suspended in phosphate-buffered saline. Survival is expressed as a percentage, using untreated cells as the 100% value.

DNA Substrates and Proteins—Single- and double-stranded circular ϕ X174 DNA was purchased from New England Biolabs. Linear ϕ X174 DNA with a unique 3'-tail (603 nucleotides in length) was constructed by PstI digestion of gapped circular φX174 DNA containing a 603-bp region of ssDNA, which was produced as follows: the 4783-bp PstI-ApaLI restriction fragment of φX174 DNA was isolated by centrifugation on a neutral 5-20% sucrose gradient as described previously (27). This fragment was heat-denatured, and the complementary strand was annealed to circular (+) ssDNA of ϕ X174, followed by purification of the gapped DNA by agarose gel electrophoresis and electroelution. The gapped DNA was precipitated, resuspended in 10 mm Tris-HCl, pH 8.0, 1 mm EDTA (TE), and dialyzed against TE for 24 h at 4 °C. The 52-mer oligonucleotide EV044 used in this study is complementary to nucleotides 130-181 of the single-stranded (+) form of φX174 DNA. Gelpurified oligonucleotides were purchased from Proligo. DNA substrates were 5'- 32 P-end-labeled using polynucleotide kinase and [γ - 32 P]ATP. Single-stranded ϕ X174 DNA was ³²P-labeled as described (28). All DNA concentrations are expressed in moles of nucleotides.

Cisplatination of XhoI-cut ϕ X174 dsDNA was carried out in a 100- μ l reaction containing 10 mm Tris-HCl, pH 7.5, 5 mm NaCl, with 5 μ g of DNA and appropriate cisplatin:DNA molar ratios by incubating at 37 °C for 16 h in the dark. Unreacted cisplatin was removed by dialysis against TE at 4 °C.

Expression and Purification of Recombinant RDM1—Plasmid pEVD008 was constructed by subcloning the chicken RDM1 gene into the Escherichia coli expression vector pET15b (Novagen).

Recombinant chicken RDM1 protein was purified from 3.2 liters of E. coli BL21(DE3)trxB⁻ (29) (a kind gift from A. Pluckthum and P. Lindner) carrying plasmid pEVD008. Cells were grown at 37 °C in Luria broth containing 60 μ g/ml ampicillin and 25 μ g/ml kanamycin to an A_{600} of 0.5 and induced by the addition of 1 mm IPTG, followed by a further 2-h incubation at 30 °C. Cells were harvested by centrifugation and resuspended in 40 ml of T buffer (20 mm Tris-HCl, pH 8.0, 0.5 m NaCl, 10% (v/v) glycerol, 0.02% (v/v) Triton X-100) containing 5 mm imidazole, frozen rapidly in liquid nitrogen, and stored at -80 °C. Bacteria were thawed and lysed by sonication in the presence of phenylmethylsulfonyl fluoride (1 mm), aprotinin (2 μg/ml), and leupeptin (2 μg/ml). Cell debris and insoluble materials were removed by centrifugation at 40,000 rpm for 45 min in a Beckman 50.2 Ti rotor. The supernatant was passed through a $0.45-\mu m$ filter and loaded onto a 40-ml Talon (Clontech) column equilibrated with T buffer containing 5 mM imidazole. The column was washed successively with 240 and 120 ml of T buffer containing 5 and 25 mm imidazole, respectively, and RDM1 was eluted with a 400-ml linear gradient of 0.025–1 $\mbox{\scriptsize M}$ imidazole in the same buffer. To prevent possible contaminations from E. coli exonuclease I (30), fractions containing RDM1 (identified by SDS-PAGE) were pooled, dialyzed against R buffer (20 mm Tris-HCl, pH 8.0, 1 mm EDTA, 0.5 mm dithiothreitol, 10% glycerol) containing 50 mm KCl, and loaded onto a 14-ml heparin-Sepharose 6 (Amersham Biosciences) column equilibrated with the same buffer. The column was washed with 400 ml of R buffer containing 50 mm KCl before a 400-ml linear gradient of 0.05-1 m KCl in R buffer was applied. Fractions containing RDM1 were dialyzed against R buffer containing 100 mm KCl (R100) and loaded onto a 20-ml Q-Sepharose column (Amersham Biosciences). The column was washed with 100 ml of the same buffer, and the protein was eluted with a 200-ml linear gradient of 0.1-1 M KCl in R buffer. RDM1 was dialyzed against R100 and loaded onto a 1-ml MonoQ (Amersham Biosciences) column equilibrated with the same buffer. The column was washed with R100, and a linear gradient of 0.1-1 M KCl in R buffer was applied. The RDM1 protein, which eluted at ~350 mm KCl, was dialyzed against R100 and stored at -70 °C. Protein concentrations were

determined using the Bio-Rad protein assay kit and bovine serum albumin as standard. The final yield of RDM1 was about 3 mg. Protein dilutions were made in R100 buffer.

DNA Binding Assays—Reactions (20 μ l) contained the ³²P-labeled DNA substrates in a standard binding buffer (20 mm MES, pH 6.4, or 20 mm sodium acetate, pH 6.0, 1 mm dithiothreitol). After 5 min at 37 °C, 1 μ l of RDM1 protein (or R100 buffer) was added, and incubation was continued for a further 10 min. Complexes were fixed by addition of glutaraldehyde (final concentration of 0.2% (v/v)) followed by 15 min of incubation at 37 °C. Protein-DNA complexes were resolved by electrophoresis through 0.8% agarose gels run in TAE buffer (or, in the case of oligonucleotide substrates, 10% polyacrylamide gels in TBE buffer), dried onto filter paper, and visualized by autoradiography.

In preliminary experiments, no protein-DNA complexes were detected when unfixed reactions with the 52-mer oligonucleotide were analyzed by gel-shift assays, as these were found to dissociate even under conditions of low ionic strength electrophoresis (data not shown). Therefore, glutaraldehyde was added to all the binding reactions analyzed in this study. It should be noted, however, that unfixed complexes assembled on larger substrates (ss and ds ϕ X174 DNA) were more stable and resulted in binding patterns identical to those observed with fixed complexes (data not shown).

Electron Microscopy—Binding reactions were fixed by addition of glutaraldehyde to 0.2%, followed by 15 min of incubation at 37 °C. Samples were then diluted and washed in 5 mm Mg(OAc)₂ before uranyl acetate staining as described previously (31). Complexes were observed using a Philips CM100 electron microscope.

Northern Blot Analysis—A multiple tissue Northern blot with each lane containing $\sim 2~\mu g$ of poly(A)+ RNA from specific tissues was purchased from Clontech. The membrane was hybridized with a 32 P-labeled probe corresponding to the human RDM1 open reading frame according to the manufacturer's instructions. A human β -actin cDNA probe (Clontech) was used as a loading control.

RESULTS

Identification and Cloning of the Chicken and Human RDM1 Genes—A database of chicken bursal ESTs has been established as a resource for the analysis of vertebrate gene function (32). While searching this database for candidate genes involved in DNA repair and/or recombination, we identified an EST whose deduced as sequence displayed partial similarity to an N-terminal region of the RAD52 protein (see below). Rapid amplification of cDNA ends was used to isolate the full-length cDNA of this gene, revealing a single open reading frame (ORF) of 277 aa (Fig. 1A). Further analysis indicated that the sequence similarity between this protein and RAD52 was restricted to a short stretch of aa, hereafter called the RD motif (see below). Because this motif was located in an important region of RAD52, and to reflect its presence in the newly identified gene, we named this gene RDM1 (for RAD52 Motif 1).

Exons of the human *RDM1* gene were first identified in genomic DNA databases using TBlastN and the chicken gene as query. The complete human *RDM1* gene, encoding a 284-aa polypeptide, was subsequently isolated by PCR, both from a testis and a brain cDNA library. Identical ORFs were amplified in both cases (data not shown). The human *RDM1* gene is located in region q11.2 of chromosome 17.

Finally, a search of SwissProt/TREMBL databases using BLAST identified a mouse protein (Q9CQK3, RIKEN cDNA clone 2410008M22) sharing significant sequence similarity with chicken and human RDM1 (see below).

Sequence Analysis of the RDM1 Proteins—A multiple sequence alignment of human (284 aa), mouse (281 aa), and chicken (277 aa) RDM1 proteins is shown in Fig. 1A. Human RDM1 was found to display 71.1 and 51.2% identity and 78.9 and 62.6% similarity, respectively, with its murine and chicken homologs.

When used to query the PFAM library of protein domains, the RDM1 sequences revealed the presence, in their N-terminal part, of a nucleic acid-binding motif of the RRM type (Fig. 1B). RRM signatures are found predominantly in various RNA-and ssDNA-binding proteins (34–36), but their interaction

with duplex DNA has also been reported (37). It is interesting to note that in human RDM1, the RRM motif corresponds exactly to exon 2 (data not shown).

We next investigated the sequence similarity between the RDM1 and RAD52 proteins. Human and yeast RAD52 proteins form multimeric ring structures that interact with ssDNA to mediate single-strand annealing (SSA) as well as RAD51-dependent and -independent strand invasion mechanisms (Refs. 20 and 38 and references therein, 39 and 40). It has been proposed that the ssDNA bound by RAD52 is exposed around the outside of the ring (41, 42). Recently, the crystal structure of RAD52 variants proficient in SSA was solved (43, 44), providing further insights into the mechanisms by which RAD52 rings interact with DNA. In a preliminary analysis, the sequence similarity shared by the RDM1 and RAD52 proteins was found to be restricted to an N-terminal region of RAD52 containing its ssDNA binding and ring formation domains. We next analyzed representative sequences of both families using MEME, a program that detects over-represented sequence motifs in unaligned sequences (45, 46). A statistically significant $(E \text{ value } 3.5 \times 10^{-75})$ 29-residue-long sequence motif shared by all sequences was identified (Fig. 1C). This motif, which we have named RD motif, spans residues 101-130 in chicken RDM1 and residues 104-133 in human and mouse RDM1. The precise location of ssDNA at the surface of a RAD52 ring is still unknown for lack of a co-crystal. However, the ssDNA is most probably bound within a deep groove that runs continuously around the outside of the ring (44). We noted that the Nterminal strand of the identified motif (aa 61-65) was part of a hairpin structure that comprises part of the proposed DNAbinding groove (Fig. 1D). Other residues of the RD motif take part in the interaction between the RAD52 monomers. For example, Phe-79 whose aromatic character is conserved in both RAD52 and RDM1 proteins forms a hydrophobic cluster with aa Leu-115, Tyr-81, Phe-158, and Tyr-31 of the adjacent monomer. Likewise, residues of helix 69-78 are in contact with residues of the adjacent monomer.

Finally, we noted the presence of Cys-127 in the RD motif of human RDM1, although a Trp was present at this position in the other proteins of Fig. 1C. However, databases of single nucleotide polymorphisms report a Cys/Trp polymorphism at this position in human RDM1, with an allele frequency of ~ 0.8 T (Cys) and ~ 0.2 G (Trp) (NCBI SNP cluster ID, rs2251660; JSNP ID, IMS-JST047036).

Disruption of RDM1 in Chicken DT40 Cells Confers Increased Sensitivity to Cisplatin—To investigate the role of RDM1 in DNA repair and recombination, we decided to disrupt it in the chicken B cell line DT40, whose genome can easily be modified by targeted recombination. To this end, we used a DT40 clone (DT40Cre1) containing a tamoxifen-inducible Cre recombinase (MerCreMer) gene that can excise loxP-flanked (floxed) cassettes. Two RDM1 knock-out constructs (pRdm1Bsr and pRdm1Puro, harboring a blasticidin and a puromycin resistance marker, respectively) were made by cloning genomic fragments of the chicken RDM1 locus upstream and downstream of floxed drug resistance markers (Fig. 2A). Targeted integration of these constructs was expected to delete nearly half of the RDM1 coding region (from codon 66 to 181).

Following transfection of pRdm1Bsr into DT40Cre1, a heterozygous RDM1 clone was identified (DT40 $RDM1^{+/-}$), which was subsequently transfected by pRdm1Puro to produce a homozygous RDM1 knock-out clone (DT40 $RDM1^{-/-}$) (Fig. 2A), indicating that RDM1 is not an essential gene. Both the blasticidin and the puromycin resistance markers were then removed from DT40 $RDM1^{-/-}$ by induction of the Cre recombi-

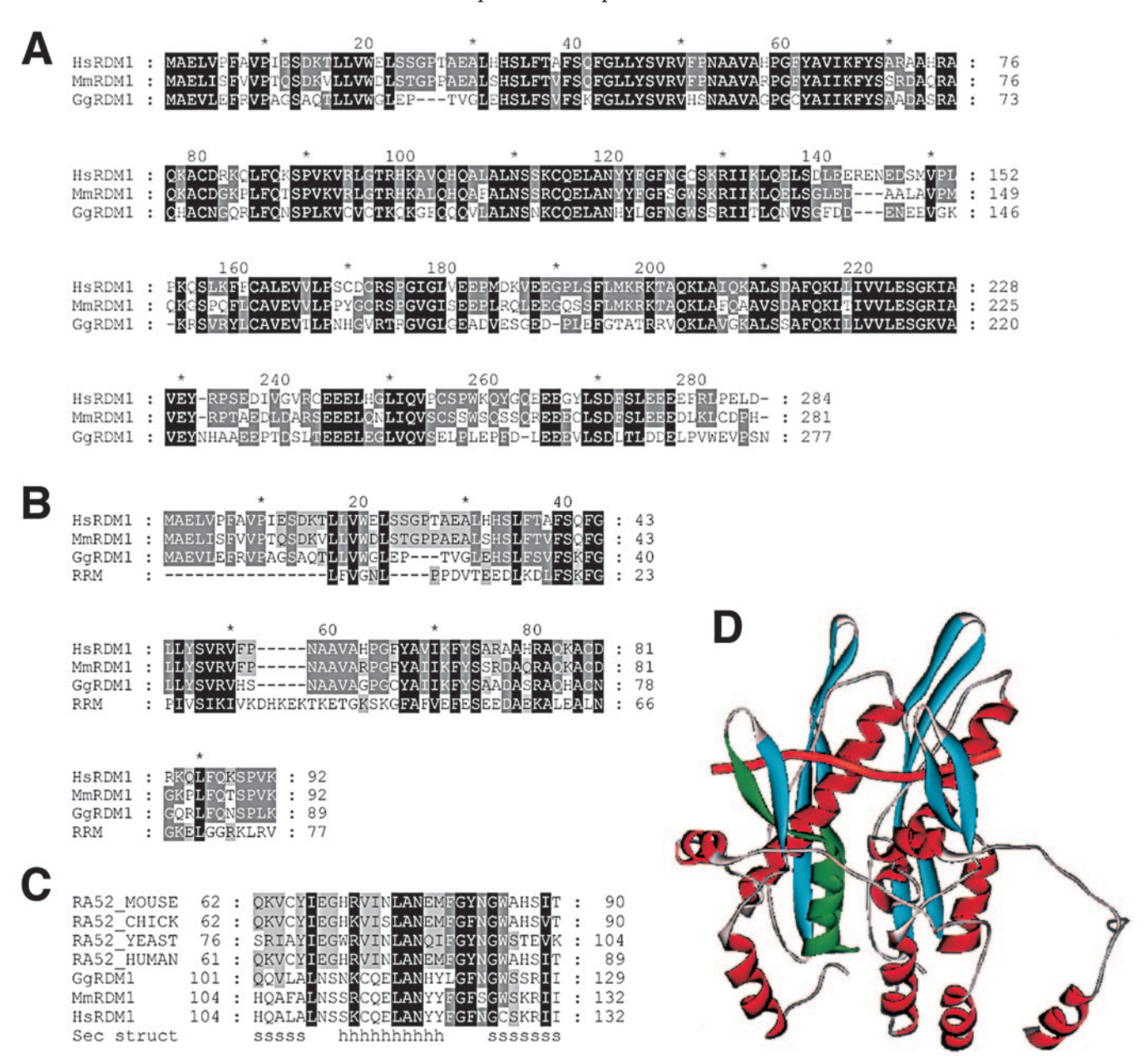


FIG. 1. Sequence analysis of the RDM1 proteins. A, protein sequence alignment of human (HsRDM1), mouse (MmRDM1), and chicken (GgRDM1) proteins performed with ClustalX (33) (default parameters). Invariant and well conserved residues are highlighted in black and gray, respectively. B, alignment of the putative RRM motif found in RDM1, with the consensus RRM sequence. Consensus residues conserved in all three proteins are highlighted in black. Conserved residues are highlighted in gray. Similar residues are shaded in gray. C, alignment of the conserved motif identified by MEME in the RDM1 and RAD52 proteins. RAD52 proteins from human, mouse, chicken, and Saccharomyces cerevisiae were used for the analysis. Secondary structures were assigned according to the crystal structure of human RAD52. Identical residues are highlighted in black. Most conserved residues with a frequency of occurrence >30% are highlighted in gray. Similar residues are shaded in gray. D, location of the RD motif in the crystal structure of human RAD52 (Protein Data Bank code 1KNO). Displayed is a ribbon representation of two adjacent monomers in a RAD52 ring. The RD motif within the first monomer is colored in green. A tubular representation of ssDNA in its proposed binding site is overlaid in orange. See text for details.

nase, yielding the clone DT40 $RDM1^{-/-E}$ (where E indicates excised). The disruption of RDM1 and the excision of the drug resistance marker were confirmed by Southern blot analysis (Fig. 2B).

The overall growth of $RDM1^{-/-E}$ cells was found to be comparable with that of wild-type cells. To examine the importance of RDM1 for DNA repair, we examined the viability of cells challenged with a variety of DNA-damaging agents using colony survival assays. For comparison purposes, we also used a DT40 cell line deficient in RAD54, a gene involved in HR and DSB repair (11, 47–49). Cells were cultured in methylcellulose plates either in the presence of cisplatin (DNA cross-linking agent) or MMS (alkylation agent), or following exposure to

 γ -radiation (DSB inducer). Surviving colonies were counted after a period of 10 days. Ablation of RDM1 did not impair significantly the cell resistance to MMS or γ -radiation (Fig. 2C). However, compared with wild-type cells, RDM1-deficient cells consistently showed a more than 3-fold increase in sensitivity to cisplatin, as evaluated at the LD37 dose (Fig. 2C). A similar cisplatin-sensitive phenotype was observed following ablation of RDM1 in RAD52-deficient cells (data not shown). As reported previously, RAD54-deficient cells showed increased sensitivity to all three DNA-damaging agents. Finally, although $RDM1^{-/-}$ cells were hypersensitive to cisplatin, they were not hypersensitive to UV light (Fig. 2C), indicating that NER remained functional in these cells.

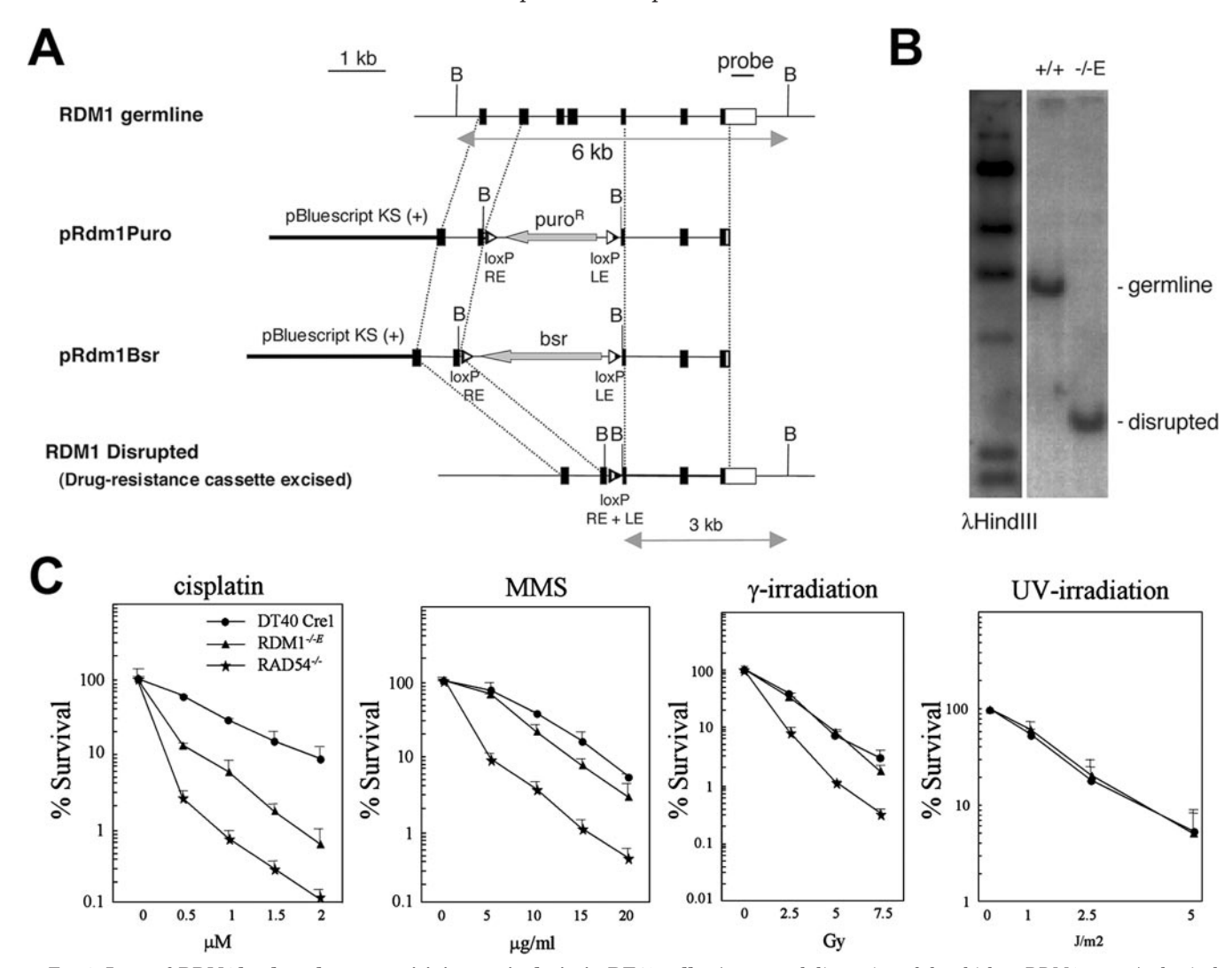


Fig. 2. Loss of RDM1 leads to hypersensitivity to cisplatin in DT40 cells. A, targeted disruption of the chicken RDM1 gene. A physical map of the RDM1 locus, the two RDM1 knock-out constructs, and the targeted loci are shown. $Open\ boxes$ represent 5'- and 3'-untranslated regions; $closed\ boxes$ represent coding regions. See text for details. B, Southern blot analysis of wild-type and RDM1-deficient DT40 cells using the probe shown in A after BamHI digestion. C, colony survival assay of wild-type, RDM1-deficient, and RAD54-deficient DT40 cells exposed to cisplatin, MMS, γ -rays, and UVC radiation. Experiments were done in triplicate, and the results are shown with standard deviations. Gy, gray.

The DT40 cell line has been shown to diversify its immunoglobulin gene by using pseudogene-templated gene conversion (50). The DT40 Cre1 cells used in this study contain a frameshift mutation within the V region of their Ig light chain gene, which allows gene conversion to be examined by monitoring the reversion of surface IgM-negative (sIgM(-)) cells to a positive status (sIgM(+)). When analyzed by this assay, gene conversion in RDM1-deficient cells was found to be comparable with that of wild-type cells (data not shown).

We next examined whether *RDM1*-deficient DT40 cells were proficient in HR by measuring gene targeting at the *MSH2* loci. By using a specific construct to target these loci, we found that HR-mediated integration reached more than 95% in wild-type DT40 cells (data not shown), consistent with previous findings (51, 52). Ablation of *RDM1* did not affect this percentage (data not shown).

Expression and Purification of Chicken RDM1 Protein—To allow the overexpression of chicken RDM1 with an N-terminal His_6 tag, the chicken RDM1 gene was cloned into the pET15b expression vector and transformed into $E.\ coli$ strain BL21(DE3) $trxB^-$. Overexpression of the protein was induced by IPTG, resulting in a 36-kDa protein that was purified to apparent homogeneity by four chromatographic steps (Fig. 3, see "Experimental Procedures").

Gel-shift Analysis and Electron Microscopic Visualization of the Interaction between RDM1 and DNA—The disruption phenotype of RDM1 in DT40 cells and the presence of an RRM motif in its gene product prompted us to study the interaction of RDM1 with DNA. To this end, we first used gel mobility assays. Increasing amounts of RDM1 protein were first incubated with a 32P-labeled 52-mer oligonucleotide, followed by fixation with glutaraldehyde and PAGE. A series of protein-DNA complexes with progressively retarded mobility was observed, suggesting binding to multiple nonspecific sites (Fig. 4A). Western blot analysis was used to confirm that these bands contained RDM1, indicating a greater accumulation of RDM1 protein in complexes with lower mobility (Fig. 4B). RDM1 was able to also interact with short ssRNA oligonucleotides, resulting in gel-shift patterns identical to that observed with ssDNA (data not shown).

Interaction of RDM1 with DNA was further explored using $^{32}\text{P-labeled}$ $\phi\text{X}174$ ssDNA (5386 nucleotides) and linear $\phi\text{X}174$ duplex DNA. RDM1 displayed noncooperative binding to ssDNA, as illustrated on agarose gel by the formation of complexes with progressively reduced mobility (Fig. 4C). RDM1 was also found to interact with duplex DNA, but in this case a more cooperative binding was observed (Fig. 4D and also see Fig. 7). A detailed study of the reaction conditions required for

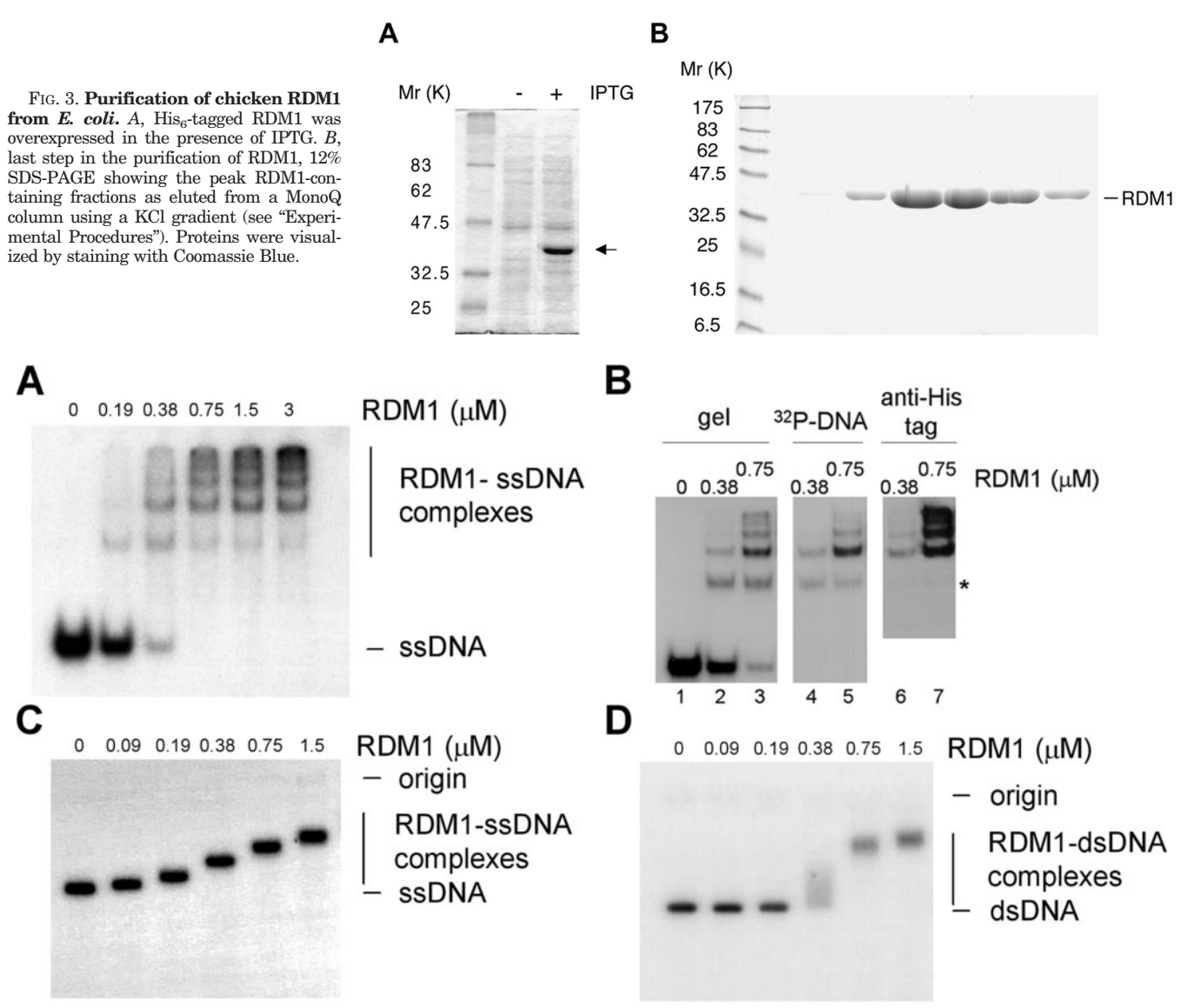


Fig. 4. Binding of RDM1 to single- and double-stranded DNA. A, the indicated concentrations of RDM1 were incubated with a 32 P-labeled 52-mer oligonucleotide (2 μ M) as described under "Experimental Procedures." Following fixation with glutaraldehyde, protein-DNA complexes were analyzed by PAGE and visualized by autoradiography. B, analysis of RDM1-ssDNA complexes with His tag antibodies. The 32 P-labeled, 52-mer oligonucleotide (4 μ M) was incubated with the indicated concentrations of RDM1. Reactions identical to those shown in lanes 2 and 3 were transferred onto a membrane (lanes 4–7), which was probed with anti-His tag monoclonal antibodies using the ECL Western blotting analysis system (Amersham Biosciences) (lanes 6 and 7, 30-s exposure), followed by rinsing and analysis of the protein-DNA complexes by autoradiography (lanes 4 and 5, 4-day exposure). Note that the faint signal in the band denoted by an asterisk in lane 7 (possibly resulting from the poor accessibility of the His tag in protein-DNA complexes involving little RDM1) is clearly visible on longer exposures of the Western blot (data not shown). C and D as described for A, except that RDM1 was incubated with 3 μ M single-stranded ϕ X174 DNA (C) or 6 μ M duplex ϕ X174 DNA (D), and complexes were analyzed by agarose gel electrophoresis.

DNA binding will be presented elsewhere.²

To visualize the products of binding reactions by electron microscopy, ssDNA-RDM1 and dsDNA-RDM1 complexes were fixed with glutaraldehyde and stained with uranyl acetate. When incubated with ssDNA, low amounts of RDM1 led to equal distribution of the protein among the DNA molecules and its random spacing along each DNA string (Fig. 5A). More active protein preparations revealed denser coating of the DNA and the appearance of small aggregates (Fig. 5B). Aggregation was found to increase with the protein concentration (Fig. 5C), resulting in higher order structures where aggregates were seen, in small numbers (4–8) and of roughly equal size, on each DNA molecule (Fig. 5D). These globular structures were separated by regions of DNA that were themselves coated by RDM1

(for example, see arrows in Fig. 5, C and D), suggesting that they originated by aggregation of RDM1-ssDNA complexes mediated by protein-protein interaction.

Interaction of RDM1 with duplex DNA (BamHI-linearized pBluescript II SK-) resulted in complexes that contrasted with those obtained using ssDNA. Little binding was observed in reactions using small concentrations of RDM1; some DNA molecules remained naked, whereas others harbored a small protein aggregate that was found at a random position along their length (Fig. 6A). When the RDM1 concentration was increased, we started to observe filament-like structures that were dispersed along the DNA, leaving regions of protein-free DNA (Fig. 6B). At higher protein concentrations, progressive coating of the DNA was observed (Fig. 6, C and D). These observations are consistent with the binding pattern observed using gel-shift assays, supporting the notion that RDM1 exhibits some degree

² S. Hamimes and E. Van Dyck, manuscript in preparation.

Fig. 5. Electron microscopic visualization of complexes made by RDM1 on single-stranded DNA. Reactions contained ϕ X174 ssDNA (3 μ M) and the following concentrations of RDM1: 0.2 μ M (A and B), 0.4 μ M (C), and 0.8 μ M (D). Note that the complexes in A and B were obtained with two different preparations of RDM1. Arrows point to RDM1-covered regions that separate the higher order structures seen at high protein concentrations. Complexes were fixed with glutaraldehyde and visualized after negative staining. The $magnification\ bar\$ denotes 40 nm.

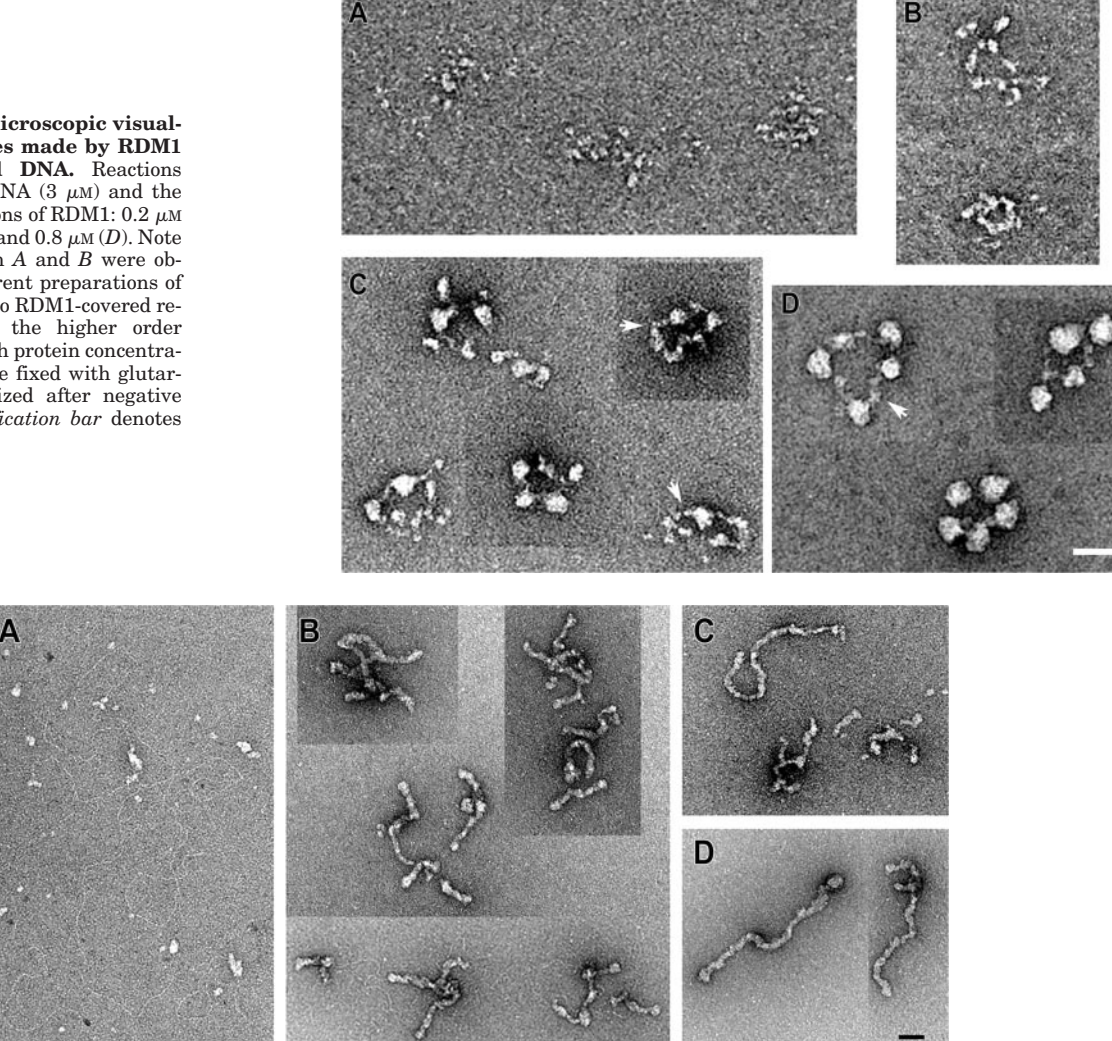


FIG. 6. Electron microscopic visualization of complexes made by RDM1 on double-stranded DNA. Reactions contained linear dsDNA (9.2 μM) and the following concentrations of RDM1: 0.2 μM (A), 0.4 μM (B), 0.8 μM (C), and 2 μM (D). The magnification bar denotes 40 nm.

of cooperativity in binding to dsDNA.

Targeting of RDM1 to Sites of Cisplatin-DNA Damage—To investigate further the mechanisms by which RDM1 confers resistance to cisplatin, we examined its binding to cisplatindamaged DNA. To this end, 32 P-labeled, linear ϕ X174 dsDNA was modified with two concentrations of cisplatin and used in gel-shift assays with increasing amounts of protein (Fig. 7A). Compared with untreated DNA, interaction of RDM1 with cisplatin-modified DNA was found to occur at lower protein concentrations (Fig. 7A, compare lane 2 with lanes 8 and 14), indicating preferential binding to the damaged DNA. Moreover, in contrast to undamaged control DNA, the most extensively modified substrate resulted in a noncooperative binding pattern (Fig. 7A, lanes 13-18), which is reminiscent of that described with ssDNA (Fig. 4B). Taken together, these observations suggest the targeting of RDM1 to randomly distributed cisplatin-DNA lesions. Consistent with this view, less extensive modification of the substrate resulted in an intermediate binding pattern where some degree of cooperativity was still apparent (Fig. 7A, lanes 7-12), indicating that the excess protein interacts with duplex DNA, when a limited number of DNA lesions are available to recruit RDM1. Because this cooperative interaction is observed at lower RDM1 concentrations compared with intact DNA (Fig. 7A, compare lane 2 with lane 8), we suggest that RDM1-bound lesions serve as preferred nucleation points for filament extension into the adjoining intact duplex. To test the hypothesis that RDM1 was targeted to sites of DNA damage, we visualized its interaction with cisplatin-modified DNA by electron microscopy. Remarkably, images obtained with the extensively modified substrate revealed that each DNA molecule was decorated with multiple protein associates (Fig. 7B). The number and distribution of these complexes most likely reflect the recognition of sites of cisplatin-DNA damage by RDM1, because at this protein concentration, untreated DNA was hardly bound by RDM1 (data not shown). Finally, higher concentrations of RDM1 resulted in the assembly of filament-like structures both on cisplatin-modified and untreated DNA (data not shown).

Interactions of RDM1 with Tailed DNA—In vertebrate cells, HR contributes to the repair of DNA ICLs (11). Single-stranded DNA tails, which serve as a scaffold for the assembly of various recombination factors, are crucial for recombinational repair, leading to the formation of nucleoprotein filaments and their invasion into a homologous duplex (40, 53, 54). The different binding patterns observed with ss- and dsDNA on gel shifts (Fig. 4) did not allow us to determine whether RDM1 binds preferentially to single-stranded regions. We therefore investigated the interaction of RDM1 with ϕ X174 DNA molecules containing a unique ssDNA tail, 603 nucleotides in length. Low amounts of RDM1 were first incubated with tailed DNA, and the resulting complexes were analyzed by electron microscopy. Remarkably, several DNA molecules with only their unique

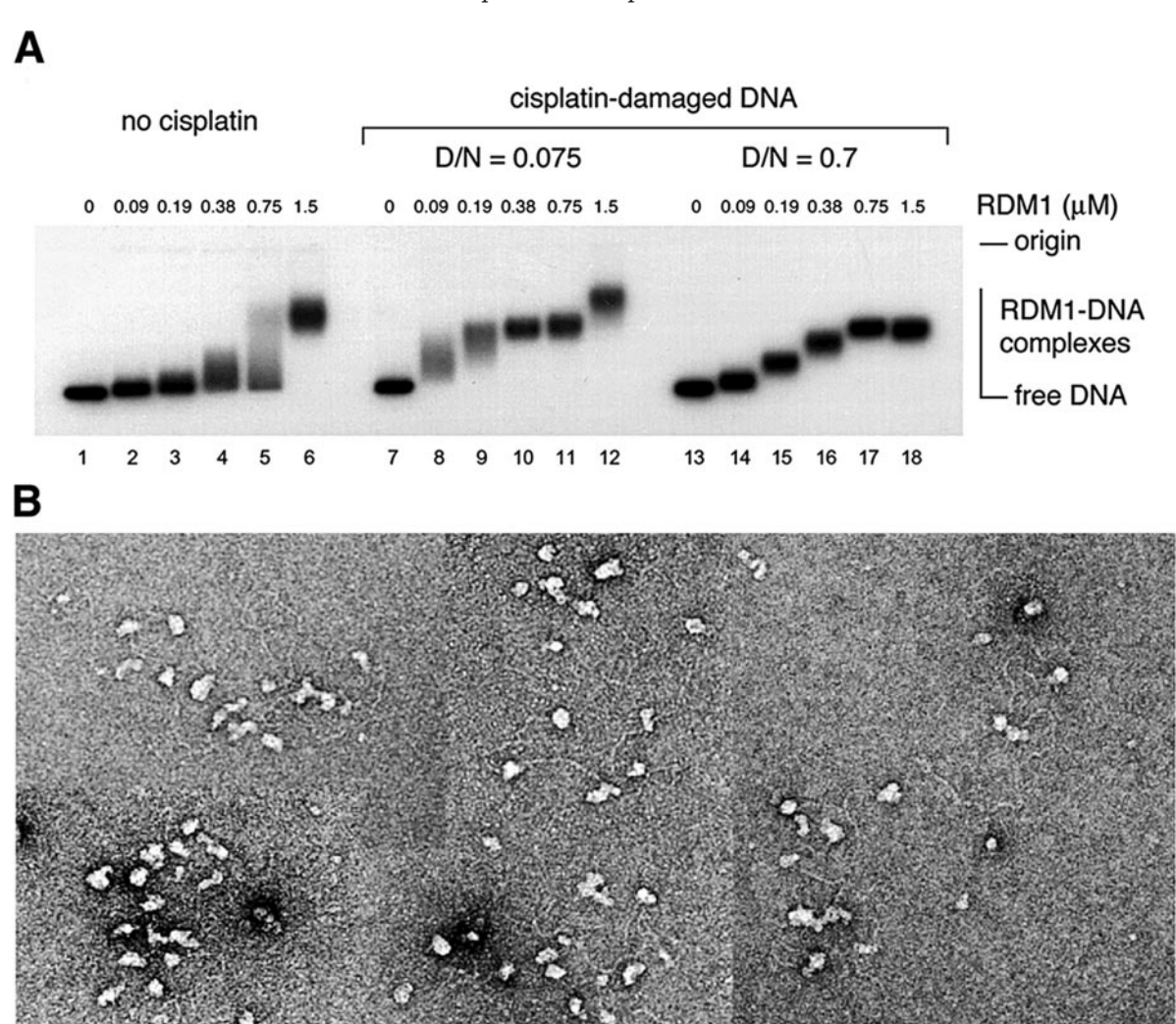


Fig. 7. Interaction of RDM1 with cisplatin-modified DNA. A, gel-shift analysis. The indicated concentrations of RDM1 were incubated with 32 P-labeled dsDNA (4 μ M), and fixed protein-DNA complexes were analyzed by agarose gel electrophoresis followed by autoradiography. Lanes 1–6 contain undamaged DNA. The DNA substrates in lanes 7–12 and 13–18 were treated with cisplatin at the indicated formal drug-to-nucleotide (D/N) ratio. B, targeting of RDM1 to cisplatin-DNA lesions. Electron microscopic visualization of complexes from a reaction containing 3.7 μ M linear dsDNA treated with cisplatin (D/N ratio = 0.7) and 200 nM RDM1. The magnification bar denotes 40 nm.

single-stranded tail bound by RDM1 protein could be seen (Fig. 8A). Because the single-strand region of the tailed DNA accounts for only 11% of the length of the substrate, these observations indicate that RDM1 interacts specifically with resected DSBs $in\ vitro$. When the concentration of RDM1 was increased, the protein was seen to also coat regions of the duplex (Fig. 8B), displaying cooperativity and forming filament-like structures similar to those shown in Fig. 6, B-D.

Displacement loop (D-loop) formation serves as an *in vitro* model reaction to characterize the strand invasion step of recombinational repair (40, 53, 55). The RRM-containing protein hPOMPp75/TSL has been shown previously (56) to exhibit DNA pairing activity and promote D-loop formation *in vitro*. Given the presence of an RRM in RDM1, and its ability to interact with tailed DNA, we tested whether RDM1 was capable of promoting assimilation of ssDNA into homologous supercoiled duplex DNA. However, by using both ss oligonucleotide or tailed DNA substrates, we did not observe efficient D-loop formation mediated by chicken RDM1 protein, under conditions where it interacts with ssDNA (data not shown).

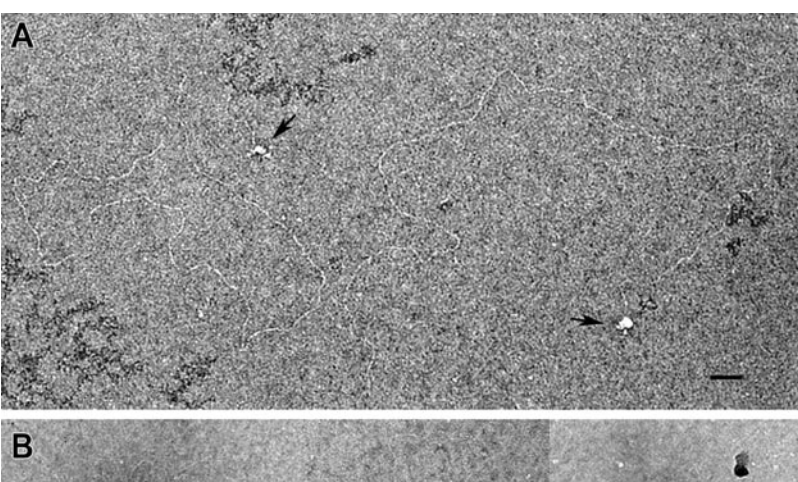
High Level Expression of Human RDM1 mRNA in the Testis— The expression pattern of human RDM1 was determined by Northern blot analysis, using mRNA from spleen, thymus, prostate, testis, ovary, small intestine, colon, and peripheral blood leukocyte (Fig. 9). A transcript of about 1200 nucleotides was detected in testis (Fig. 9, *lane 4*), whereas little or no signal was observed in the other tissues, even after a 2-week exposure. The size of this transcript is in good agreement with the length of the *RDM1* cDNA (data not shown).

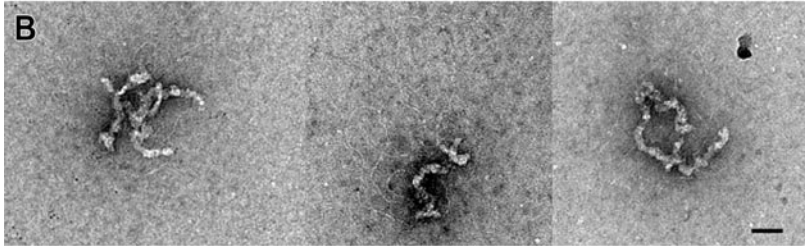
DISCUSSION

In this report, we have shown that ablation of RDM1 in chicken DT40 cells leads to an increase of their sensitivity to cisplatin. We have also revealed the DNA-binding properties of the RDM1 protein, and we demonstrated its ability to interact with cisplatin-damaged DNA $in\ vitro$. These studies provide evidence that the RDM1 gene encodes a novel factor involved in the cellular response to cisplatin.

The RDM1 protein shares a small sequence motif with members of the RAD52 protein family. The RD motif of RAD52 is located in the evolutionary conserved, N-terminal half of the protein containing its self-interaction and DNA binding domains, as well as its SSA and strand invasion activities (Ref. 20 and references therein). In addition to including the mutation rad52-1 (A90V), which originally defined RAD52 (57), the importance of the RD motif itself is underscored by a recent

Fig. 8. Electron microscopic visualization of complexes formed by RDM1 on tailed DNA. A, targeting of RDM1 to ssDNA tails. Two images from reactions containing 3 μ M linear duplex DNA with a unique ssDNA tail (603 nucleotides) and 90 nm RDM1. Black arrows point to the RDM1-bound single-stranded regions. B, filament-like structures observed in reactions containing 3 μ M tailed DNA and 375 nm RDM1. Complexes were fixed with glutaraldehyde and visualized after negative staining. Magnification bars denote 40 nm.





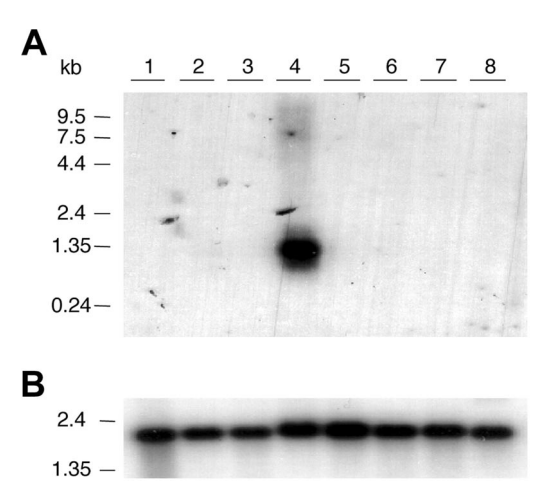


Fig. 9. Northern blot analysis of human RDM1. The following human tissues were used: $lane\ 1$, spleen; $lane\ 2$, thymus; $lane\ 3$, prostate; $lane\ 4$, testis; $lane\ 5$, ovary; $lane\ 6$, small intestine; $lane\ 7$, colon (no mucosa); $lane\ 8$, peripheral blood leukocyte. A, the membrane was hybridized with a probe corresponding to the hRDM1 ORF and exposed for 2 weeks. Note that human RDM1 transcripts are already detected in testis after 2 days (data not shown). B, the membrane was hybridized with a human β -actin probe and exposed for 4 h.

molecular genetic dissection of yeast RAD52, showing that the residues of this motif form a functionally important cluster, where mutations result in severe phenotypes (58). RAD52 crystal structure analysis (43, 44) and a recent alanine-scanning mutagenesis of human RAD52 (59) have revealed a potential function for residues of the RD motif both in ssDNA binding and the interaction between monomers. We therefore postulate that the RD motif of RDM1 plays a role in the interaction of the protein with nucleic acids, possibly as a modulator of the RRM, and/or that it is involved in the ability of RDM1 to self-interact, as illustrated in this study by the filament-like structures observed on dsDNA.

Differences were observed when we analyzed the binding of RDM1 to either single- or double-stranded DNA. We found that RDM1 bound ssDNA preferentially but with no cooperativity. In contrast, a more cooperative binding mode, resulting in the formation of filament-like structures, was displayed in the presence of duplex DNA. It is likely that the DNA binding

activities of RDM1 are mediated at least in part by its RRM motif. In addition, it is possible that other regions contribute to the DNA binding activities of RDM1. For reasons discussed above, a prime candidate for such a role is the RD motif. Whether the different binding modes displayed by RDM1 reflect selective functions during DNA damage repair and/or different roles in the metabolism of nucleic acids remains to be elucidated. Finally, one of our main findings is that RDM1 is targeted to sites of cisplatin-DNA damage *in vitro*. Because cisplatin-DNA adducts result in large distortion and unwinding of the double helix (1), it is likely that the interaction between RDM1 and cisplatin-altered DNA is mediated in part by the single-stranded character of the damaged sites.

The presence of an RRM in RDM1 but not RAD52 is but one example of the differences that exist between these proteins, as RDM1 also appears quite different from RAD52 with respect to biochemical and DNA-binding properties. Thus, the structures assembled by RDM1 on DNA, notably the filament-like structures and higher order structures, are quite unlike those described for RAD52 (Refs. 20 and references therein, 28, 38 and references therein, and 60). Likewise, although RDM1 interacts specifically with tailed DNA, no strand invasion activity was found associated to the protein *in vitro*.

Although $RDM1^{-/-}$ DT40 cells display an elevated sensitivity to cisplatin, they are not significantly impaired in the repair of MMS- and ionizing radiation-induced DNA damage, and they show no apparent defect in HR. Although we cannot exclude the existence of functional redundancies, these observations suggest that RDM1 does not contribute, directly or indirectly, to the mechanisms of base excision repair that eliminate alkylated bases (61) and to the pathways that ensure repair of DSBs induced by ionizing radiation: HR and NHEJ (19). Furthermore, NER was found to remain functional in RDM1-/- mutants. Studies of the mechanisms by which DNA interstrand cross-links are repaired have underlined the participation of components from several DNA damage repair systems (11). In particular, the presence of XPAindependent and ERCC1-XPF complex-dependent cisplatin resistance in mammalian cells (Ref. 62 and references therein) demonstrates that mechanisms other than NER also contribute to the removal of cisplatin-DNA lesions. It thus remains possible that the increased cisplatin sensitivity of *RDM1*-deficient cells reflects a role in the removal of specific DNA lesions mediated by specialized, minor repair pathways. Another possibility is that RDM1 repair functions are required only in certain chromatin contexts. Our biochemical studies indicate that RDM1 is endowed with the ability to assemble various structures on DNA, including higher order structures. It is therefore tempting to speculate that RDM1 plays a dynamic role in the context of chromatin. For instance, it is possible that RDM1 alleviates cisplatin toxicity by binding specifically to certain types of cisplatin-DNA lesions and recruiting factors to alter the architecture of the chromatin and facilitate repair. A similar hypothesis has been made for other proteins such as the functionally redundant, high mobility group box containing proteins Nhp6A and Nhp6B (63). These proteins comprise part of a nucleosome reorganizing factor (64-66), and Nhp6A has been shown to selectively bind to DNA containing a cisplatin intrastrand cross-link (63). It is interesting to note that loss of Nhp6A/B in yeast leads to an increased sensitivity to cisplatin but not UV light (63). Therefore, preferential recognition of certain types of lesions by RDM1 may also provide an explanation as to why RDM1 participates in the cell response to cisplatin without being required in the repair of UV-induced lesions. Finally, RDM1 might modulate cellular survival to cisplatin via a more indirect pathway. Studies have shown that chromatin structure has a large impact on the degree of damage caused by cisplatin (67), and it is thus possible that loss of RDM1 results in an alteration of the chromatin structure leading to an increase in accessibility of the DNA to the drug. Following the reconstitution of global NER with purified proteins (68-70), and the characterization of the DNA damage recognition factors required in vitro for this process, recent studies (10, 71-73) have also begun to unravel the mechanisms by which this pathway operates in the context of chromatin. Model repair systems using nucleosome substrates have been developed (Refs. 74-76 and references therein). Future experiments should allow us to test a requirement for RDM1 in reconstituted systems using well defined cisplatin-DNA adducts and chromatin templates.

High level expression of human RDM1 mRNA was observed in the testis, and it is therefore possible that RDM1 plays a role in spermatogenesis and/or meiotic recombination. Cisplatin has proven particularly effective in the treatment of testicular cancers (77), and it has been proposed that the good response of testicular tumors to the drug reflects their reduced capacity to repair cisplatin-DNA damage in vitro (78, 79). It will therefore be interesting to determine whether the pattern of expression of RDM1 is altered in testicular tumors, and how RDM1 contributes to the cellular resistance to cisplatin in the testis. Further studies of RDM1 in relation to the cellular response to cisplatin-DNA damage should help improve the therapeutic effectiveness of this drug against a broader range of tumors.

Acknowledgments-We are very grateful to Pierre Hainaut and Jacques Dubochet for their interest and support. We thank Stephen J. Lippard for advice regarding the preparation of cisplatinmodified DNA, Peter Karran and Claude Caron de Fromentel for critical review of the manuscript, and Georges Mollon for assistance during preparation of the figures.

REFERENCES

- 1. Wozniak, K., and Blasiak, J. (2002) Acta Biochim. Pol. 49, 583-596
- 2. Zamble, D. B., and Lippard, S. J. (1995) Trends Biochem. Sci. 20, 435-439
- Friedberg, E. C. (2001) Nat. Rev. Cancer 1, 22–33
- 4. Wood, R. D., Araujo, S. J., Ariza, R. R., Batty, D. P., Biggerstaff, M., Evans, E., Gaillard, P. H., Gunz, D., Koberle, B., Kuraoka, I., Moggs, J. G., Sandall, J. K., and Shivji, M. K. (2000) Cold Spring Harbor Symp. Quant. Biol. 65,
- 5. Bootsma, D., Kraemer, K. H., Cleaver, J. E., and Hoeijmakers, J. H. (1998) in The Genetic Basis of Human Cancer (Vogelstein, B., and Kinzler, K. W., eds) pp. 245-274, McGraw-Hill Inc., New York

- 6. Hanawalt, P. C. (2002) Oncogene 21, 8949-8956
- Reardon, J. T., and Sancar, A. (2003) Genes Dev. 17, 2539-2551
- Thoma, B. S., and Vasquez, K. M. (2003) Mol. Carcinog. 38, 1–13 9. Fitch, M. E., Nakajima, S., Yasui, A., and Ford, J. M. (2003) J. Biol. Chem. 278,
- 46906-46910 10. de Laat, W. L., Jaspers, N. G., and Hoeijmakers, J. H. (1999) Genes Dev. 13,
- 768 785
- 11. Dronkert, M. L., and Kanaar, R. (2001) Mutat. Res. 486, 217-247
- Bessho, T. (2003) J. Biol. Chem. 278, 5250-5254
- 13. Selvakumaran, M., Pisarcik, D. A., Bao, R., Yeung, A. T., and Hamilton, T. C. (2003) Cancer Res. 63, 1311-1316
- 14. Moggs, J. G., Szymkowski, D. E., Yamada, M., Karran, P., and Wood, R. D. (1997) Nucleic Acids Res. 25, 480-491
- 15. Mu, D., Tursun, M., Duckett, D. R., Drummond, J. T., Modrich, P., and Sancar, A. (1997) Mol. Cell. Biol. 17, 760–769
- 16. Yamada, M., O'Regan, E., Brown, R., and Karran, P. (1997) Nucleic Acids Res. **25,** 491–496
- 17. Massey, A., Offman, J., Macpherson, P., and Karran, P. (2003) DNA Repair (Amst.) 2, 73–89
- 18. Zhai, X., Beckmann, H., Jantzen, H. M., and Essigmann, J. M. (1998) Biochemistry 37, 16307-16315
- 19. van den Bosch M., Lohman, P. H., and Pastink, A. (2002) Biol. Chem. 383, 873-892
- West, S. C. (2003) Nat. Rev. Mol. Cell. Biol. 4, 435–445
- 21. Altschul, S. F., Madden, T. L., Schaffer, A. A., Zhang, J., Zhang, Z., Miller, W., and Lipman, D. J. (1997) Nucleic Acids Res. 25, 3389-3402
- 22. Eddy, S. R. (1998) Bioinformatics 14, 755–763
- 23. Bateman, A., Birney, E., Cerruti, L., Durbin, R., Etwiller, L., Eddy, S. R., Griffiths-Jones, S., Howe, K. L., Marshall, M., and Sonnhammer, E. L. (2002) Nucleic Acids Res. 30, 276–280
- 24. Guex, N., and Peitsch, M. C. (1997) Electrophoresis 18, 2714-2723
- 25. Arakawa, H., Hauschild, J., and Buerstedde, J. M. (2002) Science 295, 1301-1306
- 26. Arakawa, H., Lodygin, D., and Buerstedde, J. M. (2001) BMC Biotechnol. 1, 7
- Muller, B., and West, S. C. (1994) Methods Mol. Biol. 30, 413-423
- Van Dyck, E., Hajibagheri, N. M., Stasiak, A., and West, S. C. (1998) J. Mol. Biol. 284, 1027-1038
- Proba, K., Ge, L., and Pluckthun, A. (1995) Gene (Amst.) 159, 203–207
 Prasher, D. C., Conarro, L., and Kushner, S. R. (1983) J. Biol. Chem. 258, 6340-6343
- 31. Sogo, J., Stasiak, A., DeBernardin, W., Losa, R., and Koller, T. (1987) in Electron Microscopy in Molecular Biology (Sommerville, J., and Scheer, U., eds) pp. 61-79, IRL Press at Oxford University Press, Oxford
- 32. Abdrakhmanov, I., Lodygin, D., Geroth, P., Arakawa, H., Law, A., Plachy, J., Korn, B., and Buerstedde, J. M. (2000) Genome Res. 10, 2062-2069
- 33. Thompson, J. D., Gibson, T. J., Plewniak, F., Jeanmougin, F., and Higgins, D. G. (1997) Nucleic Acids Res. 25, 4876–4882
- 34. Birney, E., Kumar, S., and Krainer, A. R. (1993) Nucleic Acids Res. 21, 5803-5816
- 35. Ding, J., Hayashi, M. K., Zhang, Y., Manche, L., Krainer, A. R., and Xu, R. M. (1999) Genes Dev. 13, 1102-1115
- 36. Varani, G., and Nagai, K. (1998) Annu. Rev. Biophys. Biomol. Struct. 27, 407 - 445
- 37. DeAngelo, D. J., DeFalco, J., Rybacki, L., and Childs, G. (1995) Mol. Cell. Biol. **15,** 1254-1264
- 38. Kagawa, W., Kurumizaka, H., Ikawa, S., Yokoyama, S., and Shibata, T. (2001) J. Biol. Chem. 276, 35201–35208
- 39. Stasiak, A. Z., Larquet, E., Stasiak, A., Muller, S., Engel, A., Van Dyck, E., West, S. C., and Egelman, E. H. (2000) Curr. Biol. 10, 337-340
- 40. Sung, P., Krejci, L., Van Komen, S., and Sehorn, M. G. (2003) J. Biol. Chem. **278**, 42729-42732
- 41. Parsons, C. A., Baumann, P., Van Dyck, E., and West, S. C. (2000) EMBO J. 19, 4175-4181
- 42. Van Dyck, E., Stasiak, A. Z., Stasiak, A., and West, S. C. (2001) EMBO Rep. 2, 905-909
- 43. Kagawa, W., Kurumizaka, H., Ishitani, R., Fukai, S., Nureki, O., Shibata, T., and Yokovama, S. (2002) Mol. Cell 10, 359-371
- 44. Singleton, M. R., Wentzell, L. M., Liu, Y., West, S. C., and Wigley, D. B. (2002) Proc. Natl. Acad. Sci. U. S. A. 99, 13492-13497
- 45. Bailey, T. L., and Elkan, C. (1994) Proc. Int. Conf. Intell. Syst. Mol. Biol. 2,
- 46. Bailey, T. L., and Gribskov, M. (1998) Bioinformatics 14, 48-54
- 47. Bezzubova, O., Silbergleit, A., Yamaguchi-Iwai, Y., Takeda, S., and Buerstedde, J. M. (1997) Cell 89, 185–193
- 48. Sigurdsson, S., Van Komen, S., Petukhova, G., and Sung, P. (2002) J. Biol. Chem. 277, 42790-42794
- 49. Takata, M., Sasaki, M. S., Sonoda, E., Morrison, C., Hashimoto, M., Utsumi, H., Yamaguchi-Iwai, Y., Shinohara, A., and Takeda, S. (1998) EMBO J. 17,
- 50. Arakawa H., and Buerstedde, J. M. (2004) Dev. Dyn. 229, 458-464
- 51. Bezzubova, O. Y., and Buerstedde, J. M. (1994) Experientia (Basel) 50, 270 - 276
- 52. Buerstedde, J. M., and Takeda, S. (1991) Cell 67, 179–188
- 53. Mazin, A. V., Zaitseva, E., Sung, P., and Kowalczykowski, S. C. (2000) EMBO J. 19, 1148-1156
- 54. West, S. C., Chappell, C., Hanakahi, L. A., Masson, J. Y., McIlwraith, M. J., and Van Dyck, E. (2000) Cold Spring Harbor Symp. Quant. Biol. 65,
- 55. McIlwraith, M. J., Van Dyck, E., Masson, J. Y., Stasiak, A. Z., Stasiak, A., and West, S. C. (2000) J. Mol. Biol. 304, 151-164 56. Baechtold, H., Kuroda, M., Sok, J., Ron, D., Lopez, B. S., and Akhmedov, A. T.
- (1999) J. Biol. Chem. 274, 34337–34342 Resnick, M. A. (1969) Genetics 62, 519–531

- 58. Mortensen, U. H., Erdeniz, N., Feng, Q., and Rothstein, R. (2002) Genetics 161, 549 - 562
- 59. Lloyd, J. A., McGrew, D. A., and Knight, K. L. (2005) J. Mol. Biol. 345, 239 - 249
- 60. Ranatunga, W., Jackson, D., Lloyd, J. A., Forget, A. L., Knight, K. L., and Borgstahl, G. E. (2001) J. Biol. Chem. 276, 15876-15880
- 61. Lindahl, T. (2001) Prog. Nucleic Acids Res. Mol. Biol. 68, xvii-xxxx
- 62. Lan, L., Hayashi, T., Rabeya, R. M., Nakajima, S., Kanno, S., Takao, M., Matsunaga, T., Yoshino, M., Ichikawa, M., Riele, H., Tsuchiya, S., Tanaka, K., and Yasui, A. (2004) DNA Rep. (Amst). 3, 135–143
 63. Wong, B., Masse, J. E., Yen, Y. M., Giannikopoulos, P., Feigon, J., and John-
- son, R. C. (2002) Biochemistry 41, 5404-5414
- 64. Brewster, N. K., Johnston, G. C., and Singer, R. A. (2001) Mol. Cell. Biol. 10, 3491 - 3502
- 65. Formosa, T., Eriksson, P., Wittmeyer, J., Ginn, J., Yu, Y., and Stillman, D. J. (2001) EMBO J. 20, 3506-3517
- 66. Rhoades, A. R., Ruone, S., and Formosa, T. (2004) Mol. Cell. Biol. 24, 3907–3917
- 67. Davies, N. P., Hardman, L. C., and Murray, V. (2000) Nucleic Acids Res. 28,
- 68. Aboussekhra, A., Biggerstaff, M., Shivji, M. K., Vilpo, J. A., Moncollin, V.,

- Podust, V. N., Protic, M., Hubscher, U., Egly, J. M., and Wood, R. D. (1995) Cell 80, 859-868
- 69. Mu, D., Hsu, D. S., and Sancar, A. (1996) J. Biol. Chem. 271, 8285-8294
- 70. Mu, D., Park, C. H., Matsunaga, T., Hsu, D. S., Reardon, J. T., and Sancar, A. (1995) J. Biol. Chem. 270, 2415-2418
- 71. Birger, Y., West, K. L., Postnikov, Y. V., Lim, J. H., Furusawa, T., Wagner, J. P., Laufer, C. S., Kraemer, K. H., and Bustin, M. (2003) EMBO J. 22, 1665-1675
- 72. Green, C. M., and Almouzni, G. (2002) EMBO Rep. 3, 28-33
- 73. Green, C. M., and Almouzni, G. (2003) EMBO J. 22, 5163-5174
- 74. Hara, R., and Sancar, A. (2003) Mol. Cell. Biol. 23, 4121-4125
- 75. Wang, D., Hara, R., Singh, G., Sancar, A., and Lippard, S. J. (2003) Biochemistry **42**, 6747–6753
- 76. Ura, K., Araki, M., Saeki, H., Masutani, C., Ito, T., Iwai, S., Mizukoshi, T., Kaneda, Y., and Hanaoka, F. (2001) EMBO J. 20, 2004–2014
- 77. Masters, J. R., and Koberle, B. (2003) Nat. Rev. Cancer 3, 517-525
- 78. Koberle, B., Grimaldi, K. A., Sunters, A., Hartley, J. A., Kelland, L. R., and Masters, J. R. (1997) Int. J. Cancer 70, 551-555
- 79. Koberle, B., Masters, J. R., Hartley, J. A., and Wood, R. D. (1999) Curr. Biol.

SUPPORTING INFORMATION

Table II Exoglycosidase digestion of dual-labeled HA chains

The table shows the results of independent repeat experiments similar to those displayed in Table I.

For further information, see the text of Table I.

	xlHAS1			spHAS		
Digestion time (Hours)	[³ H]GlcA _{Free} %	[14C]GlcNAc _{Free} %	$^{3}H/^{14}C$	[³ H]GlcA _{Free} %	[14C]GlcNAc _{Free} %	³ H/ ¹⁴ C
Protocol 1						
0.5	-	-	-	7.3	36.2	0.2
1	24.5	13.8	1.8	-	-	-
1.5	-	-	-	14.5	43.7	0.3
2	38.2	23.3	1.6	-	-	-
3	-	-	-	25.2	50.1	0.5
4	36.4	30.9	1.2	-	-	-
6	58.0	71.1	0.8	38.6	55.7	0.7
Protocol 2						
0.5	-	-	-	11.5	12.8	0.9
1	11.9	17.7	0.7	-	-	-
1.5	-	-	-	15.0	19.9	0.8
2	20.4	23.0	0.9	-	-	-
3	-	-		23.4	34.4	0.7
4	30.6	31.1	1.0	-	-	-
6	37.9	29.7	1.3	34.4	49.8	0.7

^{a)}Expressed as percent of total ³H and ¹⁴C label recovered after gel chromatography (see Fig. 3).

RDM1, a Novel RNA Recognition Motif (RRM)-containing Protein Involved in the Cell Response to Cisplatin in Vertebrates

Samia Hamimes, Hiroshi Arakawa, Alicja Z. Stasiak, Andrzej M. Kierzek, Seiki Hirano, Yun-Gui Yang, Minoru Takata, Andrzej Stasiak, Jean-Marie Buerstedde and Eric Van Dyck

J. Biol. Chem. 2005, 280:9225-9235. doi: 10.1074/jbc.M412874200 originally published online December 14, 2004

Access the most updated version of this article at doi: 10.1074/jbc.M412874200

Alerts:

- · When this article is cited
- When a correction for this article is posted

Click here to choose from all of JBC's e-mail alerts

This article cites 77 references, 40 of which can be accessed free at http://www.jbc.org/content/280/10/9225.full.html#ref-list-1